ELSEVIER

Crystallization kinetics of melt-spun $Fe_{83}B_{17}$ metallic glass

A.A. Soliman [a,*], S. Al-Heniti [b], A. Al-Hajry [a],
M. Al-Assiri [a], G. Al-Barakati [b]

[a] *Physics Department, King Khalid University-Faculty of Science, P.O. Box 9004, Abha, Saudi Arabia*
[b] *Physics Department, College of Science, King Abdulaziz University, P.O. Box 80203, Jeddah, Saudi Arabia*

Abstract

The $Fe_{83}B_{17}$ metallic glass ribbons were prepared by a single roller melt-spinning technique in an atmosphere of helium. X-ray diffraction (XRD), scanning electron microscopy (SEM), and Differential scanning calorimetry (DSC), were used to investigate the structural and thermal transformations of the $Fe_{83}B_{17}$ metallic glass. The activation energy of crystallization E_c was evaluated using different theoretical models. Applying the modified Johnson-Mehl-Avrami (JMA) equation reasonably suggests that the $Fe_{83}B_{17}$ crystallization process is carried out by a bulk growth in two dimensions.
© 2003 Elsevier B.V. All rights reserved.

Keywords: Crystallization kinetics; Metallic glass; Nucleation

1. Introduction

The metallic glasses of Fe and B system have attracted much attention in the field of magnetic excitations in amorphous ferromagnets since they exhibit soft ferromagnetic properties, which are applicable in a variety of devices, including transformers, sensors, magnetic tapes and recorder heads [1–6].

The magnetic structure in transition metal metalloid (TM-met) metallic glasses is a subject of considerable scientific interest. Neutron with polarization analysis [2], Mössbauer [7] and magnetization [8] measurements were performed on $Fe_{83}B_{17}$ metallic glass to deal with the microscopic arrangement of its magnetic moments. It showed an evidence for considerable canting away from a collinear ferromagnetic structure.

The amorphous alloys are metastable materials. On increase of temperature, such non-crystalline systems transform into crystalline state in course of time. From the technological application point of view, the thermal stability of the amorphous alloys is of considerable importance. The crystallization of a metallic glass upon heating can be performed in several ways. In calorimetric measurements, two basic methods can be used, isothermal and non-isothermal. However, the results of crystallization process can be interpreted in terms of several theoretical models [9,10].

The present work concerns studies on crystallization kinetics for the $Fe_{83}B_{17}$ metallic glass. The kinetic parameters of the glass-crystallization transformation were estimated under non-isothermal conditions applying three different models, namely, Kissinger [11], Augis and Bennett [12] and modified Johnson-Mehl-Avrami (JMA) [13].

2. Experimental procedure

Parent ingots of pure Fe rod (99.98%) and B crystalline pieces (99.7%) from Aldrich Chemicals Ltd. of appropriate at.% proportions were melted and thoroughly mixed in an argon-arc furnace. The metallic glass ribbon was produced by conventional chill-block melt-spinning [14], using a steel wheel with a rim speed of approximately $50\,\mathrm{m\,s^{-1}}$, under an atmosphere of helium. For structural measurements, the resulting ribbon ($\approx 25\,\mu m$ thick and $\approx 1\,mm$ wide) was wound onto a flat plate and then X-ray investigations were performed on a Philips-PW1710 vertical goniometer with a

* Corresponding author. Present address. Physics department, Faculty of Science, Ain Shams University, Abbassia 11566, Cairo, Egypt.
Tel.: +966-722-44935; fax: +966-722-90165.
E-mail addresses: Alaa_Soliman2000@hotmail.com,
ahajry@kku.edu.sa.

curved crystal monochromator using molybdenum Kα radiation λ = 0.711 Å. For scanning electron microscope (SEM) examinations, ribbons surfaces were coated by a thin Au layer using fine coat JFC-100 E ion sputter Jeol type, for 10 min at 10 mA. The surface microstructure was studied by a Jeol type JSM-1200 scanning electron microscope.

Differential scanning calorimetry (DSC) measurements were performed using a Shimadzu DSC-50 instrument on samples of ≈20 mg encapsulated in platinum pans in an atmosphere of dry nitrogen at a flow of 30 ml min^{-1}. Powdered Al_2O_3 was used as a reference material. The temperature and energy calibrations of the instrument were performed using the well known melting temperatures and melting enthalpies of high purity tin, lead, zinc and indium supplied with the instrument, giving an accuracy of ±0.1 K for the temperature and ±0.02 mW for the energy. Non-isothermal DSC curves were obtained with selected heating scan rates 10–30 K min^{-1} in the range from room temperature to beyond the crystallization exotherm.

The fraction of crystallized materials, χ, at any temperature T is given by $\chi = (A_T/A)$ where A is the total area of the exotherm between the temperature T_1 where crystallization just begins and the temperature T_2 where the crystallization is completed (Fig. 3); A_T is the area between T_1 and T as shown by the hatched portion in Fig. 3(a) [15].

A best fit for the results was calculated by the least-square method. The arithmetic mean as well as the standard deviation were calculated for the activation energies.

3. Results and discussion

Fig. 1 shows the X-ray diffraction (XRD) patterns for (a) as-prepared ribbons and (b) after DSC scans (crystallization). The XRD pattern (Fig. 1(a)) consists only of a first main broad peak and a second peak with a shoulder indicating a typical amorphous metallic glass structure. To
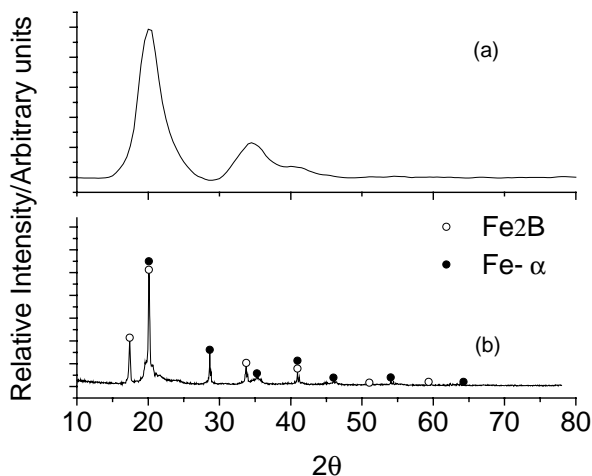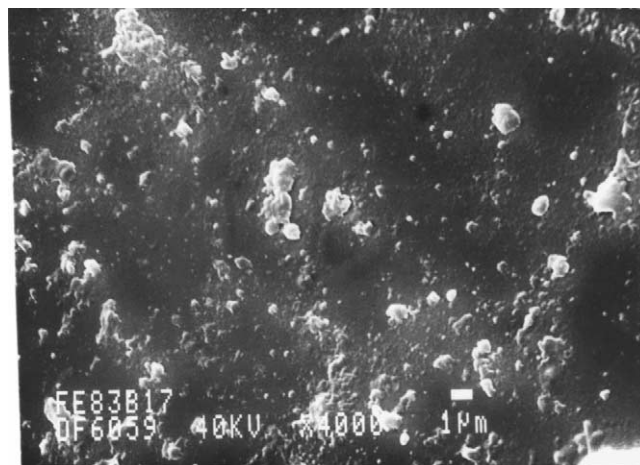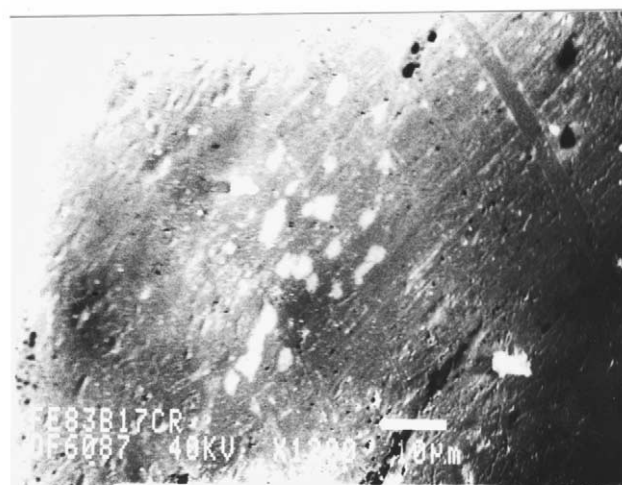

Fig. 1. X-ray diffractograms of the $Fe_{83}B_{17}$ metallic glass (a) as-prepared sample, (b) after crystallization.

Fig. 2. The SEM micrographs of the $Fe_{83}B_{17}$ metallic glass (a) as-prepared sample, (b) after crystallization.

confirm this, the as-prepared ribbon was examined using SEM (Fig. 2(a)). This figure does not show any crystalline structure, indicating that the as-prepared ribbon is completely amorphous. By analyzing the precipitated crystalline phases after crystallization (see Fig. 1(b)) the $Fe_{83}B_{17}$ metallic glass crystallizes into two phases namely the bcc-Fe of lattice constant a = 2.867 Å and the tetragonal Fe_2B (a = 5.136 Å and c = 4.380 Å). This is supported by the equilibrium phase diagram for $Fe_{100-x}B_x$ binary alloy system [16] which indicates the possibility for these two phases to form in the temperature range (27–700 °C) which is the experimental range of measurement in the present work. SEM was used to check the presence of phase separation in these metallic glass ribbons. Fig. 2(b) indicates the presence of two microcrystallites. Further work is underway to study the crystallization transformations of this system throughout the temperature range by in-situ measurements, using an X-ray diffractometer equipped with a heating stage.
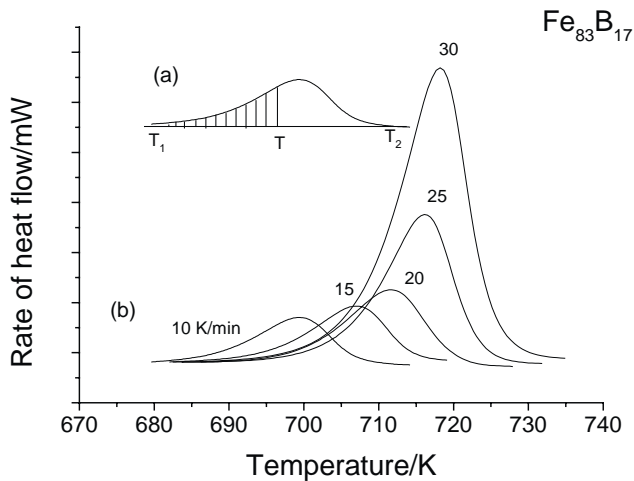
Fig. 3. Typical DSC curves at different heating rates for the $Fe_{83}B_{17}$ metallic glass.

Fig. 3 shows exothermic curves with different heating rates of the $Fe_{83}B_{17}$ metallic glass. It is clearly seen that the position of the broadening exotherm, which is associated with the crystallization, shifts towards higher temperature with the increase of the heating rate. This suggests that the crystallization process should be considered as a heating rate dependent process, which cannot be characterized by a definite critical temperature independent of the heating rate. These broadened exothermic peaks present asymmetrical profiles, which indicate the occurrence of two overlapping reactions. Therefore, it was decided to study their crystallization kinetics as a whole, as if it was a single crystallization peak.

The activation energy of crystallization (E_c) for the investigated $Fe_{83}B_{17}$ metallic glass has been estimated using the following methods.

Kissinger's method [11], which relates the dependence of the crystallization peak temperature T_p on the heating rate (α) by the following equation

$$\ln\left(\frac{\alpha}{T_P^2}\right) = -\frac{E_c}{RT_p} + \text{constant} \tag{1}$$

it was derived for the rate equation of the n th order chemical reaction, and is generally used [17–19]. However, this equation has been recently modified [20–25] to the following form

$$\ln\left(\frac{\alpha^n}{T_P^2}\right) = -\frac{mE_c}{RT_p} + \ln K \tag{2}$$

where K is a constant containing factors depending on the thermal history of the sample, and n and m are constants having values between one and four depending on the morphology of the growth. Table 1 shows the values of n and m for various crystallization mechanisms [26,27]. When nuclei form during DSC scanning, $n = m + 1$ [27]. The value of E_c is obtained from the slope of $\ln(\alpha/T_p^2)$

Table 1
Values of n and m for various crystallization mechanisms [26]

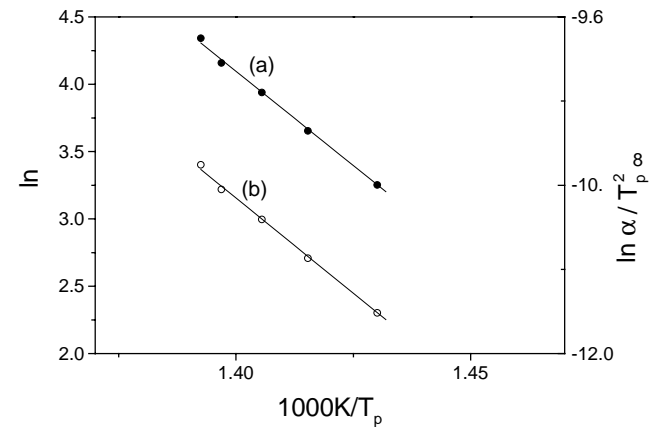| Mechanism	n	m
Bulk nucleation		
Three dimensional growth	4	3
Two dimensional growth	3	2
One dimensional growth	2	1
Surface nucleation	1	1

Fig. 4. (a) Plot of $\ln(\alpha/T_p^2)$ vs. $1000/T_p$ for the $Fe_{83}B_{17}$ metallic glass, (b) plot of $\ln(\alpha)$ vs. $1000/T_p$ for the $Fe_{83}B_{17}$ metallic glass.

versus $1/T_p$ plots given in Fig. 4(a). The obtained E_c value was $223.56 \pm 4.12\,\text{kJ}\,\text{mol}^{-1}$. For other melt-spun metallic glasses, namely, $Fe_{80}B_{20}$ [28–30], $Pd_{80}Si_{20}$ [31–33] and $Co_{75}B_{25}$ [34], the values of E_c are 202.60–260.49, 299.08–366.62 and $221.90\,\text{kJ}\,\text{mol}^{-1}$, respectively. It is a common practice also to infer $(m/n)E_c$ from the slope of $\ln(\alpha)$ versus $1/T_p$ plot itself. Fig. 4(b) shows the plot of $\ln(\alpha)$ versus $1/T_p$ data the melt-spun $Fe_{83}B_{17}$ metallic glass. The value of $(m/n)E_c$ obtained from such a plot is listed in Table 2 (column 5). To evaluate E_c, a knowledge of m and n, that is, some details of the crystallization process are necessary.

The modified Johnson-Mehl-Avrami equation concerning the kinetics of phase transformation involving nucleation and growth under isothermal conditions is generally used to analyze the crystallization process. For applicability of this equation to non-isothermal crystallization process, several conditions will have to be satisfied [9]. To check the validity of interpretation of the crystallization data obtained presently in terms of the JMA equation, the suggested

Table 2
Data on m, n and E_c for the melt-spun $Fe_{83}B_{17}$ metallic glass

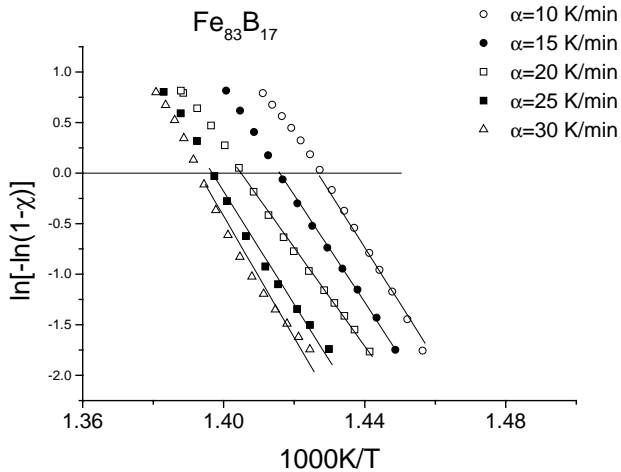| From $\ln[-\ln(1-\chi)]$ vs. $1/T$ and vs. $\ln\alpha$ data				From $\ln\alpha$ vs. $1/T_p$ data		From $\ln\alpha$ vs. $1/T_c$ data	
mE_c	n	m	E_c	$(m/n)E_c$	E_c	$(m/n)E_c$	E_c
470.50	3.25	2	235.25	137.57	223.56	136.01	221.01

Fig. 5. plot of $\ln[-\ln(1-\chi)]$ vs. $1000/T$ at three different heating rates for the $Fe_{83}B_{17}$ metallic glass.

Fig. 6. plot of $\ln[-\ln(1-\chi)]$ as a function of $\ln(\alpha)$ at three different temperatures for $Fe_{83}B_{17}$ metallic glass.

cursory check [9], namely, whether the fraction χ_p transformed at T_p is around 0.6–0.63 was used. For the present melt-spun $Fe_{83}B_{17}$ metallic glass for all the heating rates, values of χ_p at T_p are found in the range 0.60–0.63.

For non-isothermal crystallization, the volume fraction of crystals χ, precipitated in a glass heated at a uniform heating rate α is related to E_c through the following expression [13,25–27,35]

$$\ln[-\ln(1-\chi)] = -n\ln(\alpha) - \frac{1.052\,mE_c}{RT} + \text{constant} \quad (3)$$

where m and n are numerical factors already defined above. Fig. 5 shows the plot of $\ln[-\ln(1-\chi)]$ versus $1/T$ at various heating rates. This plot is found to be linear over most of the temperature range. At high temperatures or in the regions of large crystallization fractions, a slight deviation in the linearity or rather a decrease of the initial slope is observed for all heating rates. This deviation could be attributed to the saturation of the nucleation sites in the final stages of crystallization [36,37]. The other possibility to explain such a behavior could be the restriction of crystal growth by the small size of the particles [38]. Here, the analysis is restricted to the initial linear region which extends over a large temperature range [24].

The values of mE_c at different heating rates can be obtained from the slope of Fig. 5 and seemed to be independent of the heating rate. Therefore, an average of mE_c was calculated by considering all the heating rates.

The data of Fig. 5 are used to evaluate $\ln[-\ln(1-\chi)]$ as a function of $\ln(\alpha)$ for the crystallization of the as-prepared $Fe_{83}B_{17}$ metallic glass and are given in Fig. 6 at three different temperatures namely, 300, 305 and 310 K. Similarly, the value of n has been evaluated from the slopes of these relations, and the average value of n was calculated to be 3.25. For $Fe_{83}B_{17}$ metallic glass, no specific heat treatment was performed prior to the DSC scans to nucleate the sample. Therefore, n is considered to be equal to $(m + 1)$ for
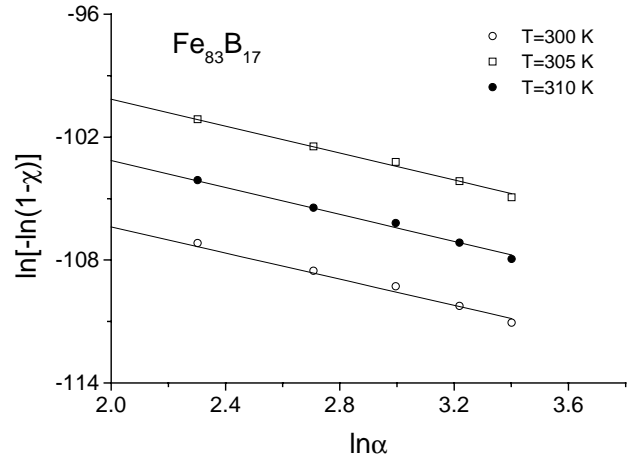
the glass. The calculated value of n is not an integer, which means that the crystallization process of $Fe_{83}B_{17}$ metallic glass occurs with different mechanisms and the predominant one is the process in which $n = 3$ [24,38]. Therefore, the value of the corresponding m is equal to 2. Therefore it is somewhat reasonable to suggest that the $Fe_{83}B_{17}$ crystallization process can be carried out by a bulk crystallization in two dimensions.

The E_c value is calculated also using the variation of T_c with the heating rate α for the crystallization of $Fe_{83}B_{17}$ metallic glass. Eqs. (1) and (2), can be rewritten in the form

$$\ln\left(\frac{\alpha}{T_c^2}\right) = -\frac{E_c}{RT_c} + \text{constant} \quad (4)$$

and

$$\ln(\alpha) = -\left(\frac{m}{n}\right)\frac{E_c}{RT_c} + \text{constant} \quad (5)$$

Fig. 7 shows plots of such relations and the deduced E_c value (averaged) for $Fe_{83}B_{17}$ crystallization is 221.01 $\pm$
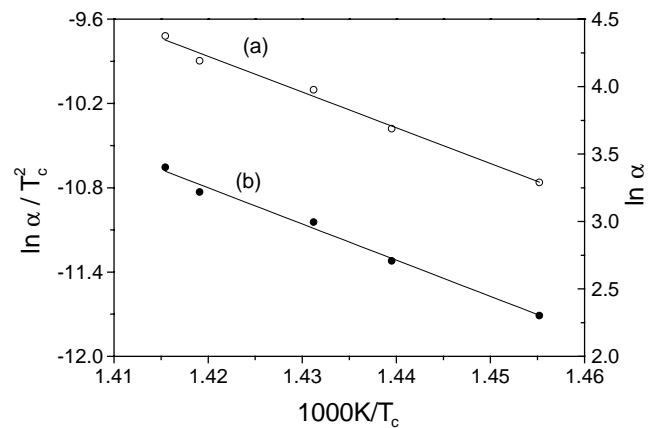

Fig. 7. (a) plot of $\ln(\alpha/T_c^2)$ vs. $1000/T_c$ for the $Fe_{83}B_{17}$ metallic glass, (b) plot of $\ln(\alpha)$ vs. $1000/T_c$ for the $Fe_{83}B_{17}$ metallic glass.
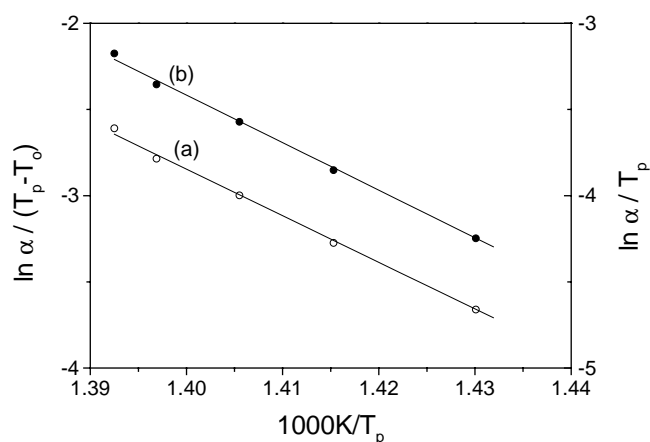
Fig. 8. (a) plot of $\ln[\alpha/(T_p - T_o)]$ vs. $1000/T_p$ for the $Fe_{83}B_{17}$ metallic glass., (b) plot of $\ln(\alpha/T_p)$ vs. $1000/T_p$ for the $Fe_{83}B_{17}$ metallic glass.

$6.28\,kJ\,mol^{-1}$ which is in good agreement with the above results.

Augis and Bennett's method [12], which gives the dependence of T_p on α in the following form

$$\ln\left[\frac{\alpha}{(T_p - T_o)}\right] = -\frac{E_c}{RT_p} + \text{constant} \qquad (6)$$

where T_o is the initial temperature (room temperature) of DSC thermal curves. Fig. 8(a) shows the relationship of $\ln[\alpha/(T_p - T_o)]$ versus $1/T_p$ (Eq. (6)). The deduced value of E_c for melt spun $Fe_{83}B_{17}$ glass, in this case, is $224.78 \pm 4.33\,kJ\,mol^{-1}$. Assuming that $T_o \ll T_p$, the relation $\ln(\alpha/T_p)$ versus $1/T_p$ gives a straight line as shown in Fig. 8(b). The calculated value of E_c, in this case, is $226.41 \pm 4.95\,kJ\,mol^{-1}$.

Values of the activation energy of crystallization of the $Fe_{83}B_{17}$ metallic glass obtained by both Kissinger and Augis–Bennett methods are reinforcing each other. The noticeable difference between the results obtained by these two models and those obtained by the JMA model could be attributed to the applicability of JMA equation to non-isothermal kinetics [9,39].

The activation energies to be considered in a crystallization process are the activation energy for nucleation (E_n), activation energy for crystal growth (E_G) and that for the whole process of crystallization, called the activation energy for crystallization denoted by E_c. The thermal analysis methods enable the determination of E_c [40,41]. It has been pointed out [42] that in non-isothermal measurements, generally due to a rapid temperature rise and big differences in the latent heats of nucleation and growth, the crystallization exotherm characterises the growth of the crystalline phase from the amorphous matrix; nucleation is more or less calorimetrically unobservable at temperatures below the crystallization exotherm, or it takes place very rapidly and immediately after overheating of the material in the initial stages of the crystallization exotherm, which results in the deformed beginning of the measured exotherm. consequently, the obtained values of E_c can be taken to represent the activation energy of growth, E_G of this melt-spun $Fe_{83}B_{17}$ metallic glass.

4. Conclusions

The XRD and SEM measurements showed that the investigated $Fe_{83}B_{17}$ metallic glass crystallizes through Fe-α and Fe_2B phases. This is consistent with the equilibrium phase diagram for $Fe_{100-x}B_x$ binary alloy system in the measured temperature range.

The calculations of the activation energy of crystallization E_c revealed that the results obtained by Kissinger and Augis–Bennett models, are in good agreement. The slight difference between E_c values obtained by both models and those obtained on the basis of JMA model could be attributed to the applicability of JMA equation to non-isothermal kinetics of the $Fe_{83}B_{17}$ metallic glass investigated. Finally, based on the modified JMA model, it can be reasonably suggested that the crystallization process of the $Fe_{83}B_{17}$ metallic glass is carried out by a bulk crystallization growth in two dimensions. The results further indicate that the activation energy (E_c) measured by non-isothermal measurements correspond to the activation energy for crystal growth (E_G) in this melt-spun $Fe_{83}B_{17}$ metallic glass.

References

[1] R.A. Cowley, D.Mck. Paul, W.G. Stirling, N. Cowlam, Physica 120B (1983) 373.
[2] R.A. Cowley, C. Patterson, N. Cowlam, P.K. Ivison, J. Martinez, L.D. Cussen, J. Phys. Condens. Matter 3 (1991) 9521.
[3] R.A. Cowley, N. Cowlam, L.D. Cusson, J. Phys. Coll. 49 (1988) 920.
[4] N. Cowlam, J. Non-Cryst. Solids 205–207 (1996) 567.
[5] A.R. Wildes, R.A. Cowley, S. Al-Heniti, N. Cowlam, J. Kulda, E. Lelièvre-Berna, J. Phys. Condens. Matter 10 (1998) 2617.
[6] S. Al-Heniti, N. Cowlam, A.R. Wildes, J. Phys. Condens. Matter 11 (1999) 9139–9150.
[7] S.J. Harker, R.J. Pollard, J. Phys. Condens. Matter 1 (1989) 8269.
[8] S.N. Kaul, P.D. Babu, Phys. Rev. B 50 (1994) 9308.
[9] D.W. Handerson, J. Non-Cryst. Solids 30 (1979) 301.
[10] H. Yinnon, D.R. Uhlmann, J. Non-Cryst. Solids 54 (1983) 253.
[11] H.E. Kissinger, J. Res. Nat. Bur. Stand. 57 (1956) 217.
[12] J.A. Augis, J.E. Bennett, J. Therm. Anal. 13 (1978) 253.
[13] K. Matusita, T. Konatsu, R. Yorota, J. Mater. Sci. 19 (1984) 291.
[14] S.H. Al-Heniti, Ph.D. thesis, University of Sheffield, UK, 1999.
[15] S. Suriñach, M.D. Baro, M.T. Clavaguera-Mora, N. Clavaguera, J. Non-Cryst. Solids 54 (1983) 253.
[16] W.G. Moffat, The Handbook of Binary Phase Diagrams, Genium Publishing, 1978.
[17] H.E. Kissinger, Anal. Chem. 29 (1957) 1702.
[18] H.S. Chen, J. Non-Cryst. Solids 7 (1978) 257.
[19] R. Frahn, J. Non-Cryst. Solids 56 (1983) 255.
[20] K. Matusita, S. Sakka, Phys. Chem. Glasses 20 (1979) 81.
[21] D.R. MacFarlane, M. Matecki, M. Poulain, J. Non-Cryst. Solids 64 (1984) 351.
[22] K. Matusita, S. Sakka, J. Non-Cryst. Solids 38–39 (1980) 741.
[23] K. Matusita, S. Sakka, Bull. Instr. Chem. Res. Kyoto Univ. 59 (1981) 159.
[24] A. Morotta, S. Saiello, A. Buri, J. Non-Cryst. Solids 57 (1983) 473.

[25] K. Matusita, S. Sakka, Thermochim. Acta 33 (1979) 351.
[26] K. Matusita, S. Sakka, Thermochim. Acta 33 (1979) 351.
[27] S. Mahadevan, A. Giridhar, A.K. Singh, J. Non-Cryst. Solids 88 (1986) 11.
[28] L.A. Davis, R. Ray, C.P. Chou, R.C. O'Handley, Sci. Metall. 10 (1976) 411.
[29] F.E. Luborsky, Mater. Sci. Eng. 28 (1977) 139.
[30] J.A. Leake, A.L. Greer, J. Non-Cryst. Solids 38/39 (1980) 735.
[31] T. Spassov, Cryst. Res. Technol. 27 (1992) 149.
[32] P. Duhaj, D. Barancok, A. Ondrejka, J. Non-Cryst. Solids 21 (1976) 411.
[33] M.A. Marcus, J. Non-Cryst. Solids 30 (1979) 317.
[34] U. Koster and U. Herold, in: H.J. Guntherodt, H. Beck (Eds.), Glassy Metals I: Topics in Applied Physics, vol. 46, Springer, 1981, p. 225.
[35] B.G. Bagley, E.M. Vogel, J. Non-Cryst. Solids 18 (1975) 29.
[36] M.G. Scott, J. Mater.Sci. 13 (1978) 291.
[37] V.R.V. Raman, G.E. Fish, J. Appl. Phys. 53 (1982) 2273.
[38] J. Colemenero, J.M. Barandiaran, J. Non-Cryst. Solids 30 (1978) 263.
[39] P. Duhaj, D. Barancok, A. Ondreika, J. Non-Cryst. Solids 21 (1976) 411.
[40] S. Ranganathan, M. von Heimendahl, J. Mater. Sci. 16 (1981) 2401.
[41] M. von Heimendahl, G. Kuglstatter, J. Mater. Sci. 16 (1981) 2405.
[42] E. Illekova, J. Non-Cryst. Solids 68 (1984) 153.